**Atmospheric
Chemistry
and Physics
Discussions**

ClOOCl photolysis at high solar zenith angles: analysis of the RECONCILE self-match flight

O. Sumińska-Ebersoldt[1], R. Lehmann[2], T. Wegner[1], J.-U. Grooß[1], E. Hösen[3], R. Weigel[4,5], C. M. Volk[3], S. Borrmann[4,5], M. Rex[2], F. Stroh[1], and M. von Hobe[1]

[1]Institute of Energy and Climate Research: Stratosphere (IEK-7), Forschungszentrum Jülich GmbH, Jülich, Germany
[2]Alfred Wegener Institute for Polar and Marine Research, Potsdam, Germany
[3]Department of Physics, University of Wuppertal, Germany
[4]Institute for Physics of the Atmosphere, Johannes Gutenberg Universität Mainz, Germany
[5]Particle Chemistry Department, Max Planck-Institute für Chemie, Mainz, Germany

Correspondence to: O. Sumińska-Ebersoldt (o.suminska@fz-juelich.de)
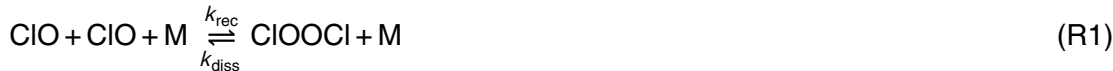
Abstract

The photolysis frequency of dichlorine peroxide (ClOOCl) J_{ClOOCl} is a critical parameter in catalytic cycles destroying ozone in the polar stratosphere. In the atmospherically relevant wavelength region, published laboratory measurements of ClOOCl absorption cross sections and spectra are not in good agreement, resulting in significant discrepancies in J_{ClOOCl}. Previous investigations of the consistency with atmospheric observations of ClO and ClOOCl have focused on the photochemical equilibrium between ClOOCl formation and photolysis, and thus could only constrain the ratio of J_{ClOOCl} over the rate constant of the ClO recombination reaction k_{rec}. Here, we constrain the atmospherically effective J_{ClOOCl} independent of k_{rec} using ClO data sampled in the same air masses before and directly after sunrise. Over sunrise, when the ClO/ClOOCl system comes out of thermal equilibrium and the influence of the ClO recombination reaction is negligible, the rise in ClO concentration is significantly faster than expected from J_{ClOOCl} based on the absorption spectrum proposed by Pope et al. (2007), but does not warrant cross sections larger than recently published values by Papanastasiou et al. (2009). In particular, the existence of a significant ClOOCl absorption band longwards of 420 nm, is effectively ruled out by our observations. Additionally, the night-time ClO observations show that the ClO/ClOOCl thermal equilibrium constant can not be significantly higher than the one proposed by Plenge et al. (2005).

1 Introduction

Once chlorine is activated on PSCs (Solomon et al., 1986) or background aerosol (Drdla and Müller, 2010) in the polar stratosphere and sunlight is available, photochemical ozone loss occurs essentially via two catalytic cycles, the ClO-dimer cycle (Molina and Molina, 1987):

$$\text{ClO} + \text{ClO} + \text{M} \underset{k_{diss}}{\overset{k_{rec}}{\rightleftharpoons}} \text{ClOOCl} + \text{M} \tag{R1}$$

$$ClOOCl + h\nu \xrightarrow{J_{ClOOCl}} Cl + ClOO \tag{R2}$$

$$ClOO + M \rightarrow Cl + O_2 + M \tag{R3}$$

$$2 \times (Cl + O_3 \rightarrow ClO + O_2) \tag{R4}$$

$$\overline{}$$

$$2O_3 + h\nu \rightarrow 3O_2$$
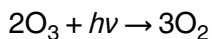
and the ClO-BrO cycle (McElroy et al., 1986):

$$BrO + ClO \rightarrow Br + Cl + O_2 \tag{R5}$$

$$Br + O_3 \rightarrow BrO + O_2 \tag{R6}$$

$$Cl + O_3 \rightarrow ClO + O_2 \tag{R4}$$

$$\overline{}$$

$$2O_3 + h\nu \rightarrow 3O_2$$
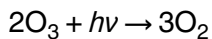
The forward and backward Reaction (R1) of the ClO-dimer cycle, i.e. the ClO recombination and the ClO dimer (ClOOCl) thermal dissociation, govern the partitioning between ClO and ClOOCl in darkness with a thermal equilibrium constant

$$K_{eq} = \frac{k_{rec}}{k_{diss}} = \frac{[ClOOCl]}{[ClO]^2}. \tag{1}$$

At daylight, Reactions (R2)–(R4) shift the ClO_x ($\approx ClO + 2ClOOCl$) partitioning towards the monomer and drive chemical ozone loss (Reaction R4). The ClOOCl photodissociation Reaction (R2) is the rate-limiting step of the ClO-dimer cycle under twilight conditions that prevail throughout most of the winter in the polar stratosphere. By governing the ClO concentration, Reaction (R2) also limits the rate of Reaction (R5)

ClOOCl photolysis at high solar zenith angles

O. Sumińska-Ebersoldt et al.

in the ClO-BrO cycle, making the ClOOCl photolysis frequency J_{ClOOCl} by far the most critical kinetic parameter for the overall ozone loss rate (von Hobe et al., 2007).

J_{ClOOCl} is a product of the ClOOCl photolysis cross section (absorption cross section $\sigma_{ClOOCl}(\lambda)$ times the photolysis quantum yield $\phi(\lambda)$, i.e. the fraction of absorbed photons leading to photodissociation; plotted in Fig. 1a) and the actinic flux $I(\lambda)$ (Fig. 1b) integrated over wavelengths:

$$J_{ClOOCl} = \int \sigma_{ClOOCl}(\lambda) \cdot \phi(\lambda) \cdot I(\lambda) \cdot d\lambda \tag{2}$$

Photolysis cross sections have been determined by monitoring the disappearance of ClOOCl (Chen et al., 2009; Lien et al., 2009; Jin et al., 2010) or the appearance of Cl atoms (Wilmouth et al., 2009) in photolysis experiments at discrete wavelengths. For the wavelength range relevant for ClOOCl photolysis in the stratosphere ($\lambda > 310$ nm), only absorption cross sections (Cox and Hayman, 1988; DeMore and Tschuikow-Roux, 1990; Burkholder et al., 1990; Bloss et al., 2001; Papanastasiou et al., 2009) or relative absorption spectra (Huder and DeMore, 1995; von Hobe et al., 2009; Pope et al., 2007) have been measured by UV/Vis absorption spectroscopy. Because excited states of ClOOCl are rapidly dissociative (Birk et al., 1989; Kaledin and Morokuma, 2000; Toniolo et al., 2001; Peterson and Francisco, 2004), absorption and photolysis cross sections are often assumed to be equivalent, i.e. $\phi(\lambda) \sim 1$.

The laboratory studies, in which absorption spectra have been measured, are lacking the knowledge of the amount of ClOOCl present in the absorption cell and the relative spectra have to be scaled to one of the following absolute cross section measurements. The studies of Cox and Hayman (1988), DeMore and Tschuikow-Roux (1990) and Burkholder et al. (1990) indicated the absorption peak value of ClOOCl at 245 nm between 5.8×10^{-18} and 7.2×10^{-18} cm^2 molecule^{-1}. According to the results of Papanastasiou et al. (2009), the absorption peak is at 244.5 nm and has a value of 7.6×10^{-18} cm^2 molecule^{-1}, Wilmouth et al. (2009) placed the photolysis peak of 6.6×10^{-18} cm^2 molecule^{-1} at 248.0 nm, whereas studies of Lien et al. (2009) showed even higher photolysis cross section (8.85×10^{-18} cm^2 molecule^{-1}) near to the

Full Screen / Esc

Printer-friendly Version

Interactive Discussion

assumed peak, at 248.4 nm. Here, we chose to scale all relative absorption spectra to the cross section of Lien et al. (2009) for two reasons:

– Lien et al. (2009) have used a novel approach in which a molecular beam of ClOOCl is attenuated through photolysis by laser light. The method is insensitive to UV absorption interference by impurities and does not require information on the absolute ClOOCl concentration,

– it seems unreasonable to scale a relative absorption spectrum to an absolute cross section associated with a different spectral shape.

The upper panel of Fig. 1 shows that the existing laboratory studies on σ_{ClOOCl} display large uncertainties especially in the long wavelength tail, i.e. in the region of most relevance in the atmosphere. These uncertainties propagate directly into the atmospheric J_{ClOOCl} values derived from the cross section measurements. Figure 1c reveals the significance of the photolysis longward of 400 nm at high solar zenith angles (SZA) and thus emphasizes the importance of the increasingly small cross sections in this wavelength region. The inability to tightly constrain J_{ClOOCl}, that governs the ClO-dimer cycle, is one of the key issues preventing full quantitative understanding of the ozone depletion in the winter/early spring polar atmosphere.

Here, we investigate four sets of ClOOCl absorption cross sections/scaled spectra (Sect. 2) and their influence on [ClO] rise at high SZA. For comparison, we use pairs of in-situ ClO measurements in the same air mass just before and after sunrise obtained during a so called self-match flight. The self-match flight pattern and the measurements are described in Sects. 3.1 and 3.2. Section 3.3 describes in detail the approach employed to test the consistency of the four different $J_{ClOOCl}(\lambda)$ values with the observed rise in ClO concentration over the sunrise. An assessment of the success in resampling the same air in the matches based on observations of a chemically and dynamically conserved tracer and the results of the ClO/ClOOCl kinetic studies will be presented in Sect. 4.

Title Page

Abstract	Introduction
Conclusions	References
Tables	Figures

◀◀   ▶▶

◀   ▶

Back   Close

Full Screen / Esc

Printer-friendly Version

Interactive Discussion

2 Investigated σ_{ClOOCl}

In further analysis two relative spectra, absolute cross sections and an artificial spectrum are considered:

    i. Pope et al. (2007) presented ClOOCl spectrum with the lowest ever published absorption cross sections at $\lambda > 310$ nm resulting in relatively small J_{ClOOCl} values. They carried out an innovative experiment purifying ClOOCl prior to the absorption measurement, thus removing all impurities other than Cl_2. However, in their spectral analysis they probably overcorrected for the Cl_2 impurity as has been shown by von Hobe et al. (2009) (see below). The spectrum is scaled to measurements of Lien et al. (2009) to obtain cross sections.

    ii. von Hobe et al. (2009) used the same technique proposed by Pope et al. (2007) to prepare and purify ClOOCl, but measured the spectrum of sample isolated in a solid noble gas matrix. In the atmospherically relevant region, their spectrum lies considerably higher than the Pope et al. (2007) spectrum but compares rather well to a Pope et al. (2007) gas phase spectrum uncorrected for Cl_2. The von Hobe et al. (2009) spectrum is also scaled to cross section of Lien et al. (2009).

    iii. Papanastasiou et al. (2009) measured absolute cross sections over a wavelength range from the ClOOCl absorption peak into the visible. The new measurement refines an earlier study from the same laboratory (Burkholder et al., 1990). The two spectra have slightly different shapes but yield similar atmospheric J_{ClOOCl} values. Burkholder et al. (1990) results generally produced the best agreement in a number of studies comparing modelled and observed ClO_x partitioning (Stimpfle et al., 2004; von Hobe, 2007; Schofield et al., 2008; Kremser et al., 2010) as well as ozone loss (Santee et al., 2003; Chipperfield et al., 2005; Frieler et al., 2006; Tripathi et al., 2006).

    iv. An artificial spectrum based on Papanastasiou et al. (2009), but with a simulated σ_{ClOOCl} set constant to 7.12×10^{-21} cm^2 molecule^{-1} above 420 nm is used to test

the possible existence of an additional ClOOCl absorption band in the visible.

J_{ClOOCl} values derived from the cross sections i–iv and the actinic flux from Fig. 1b are shown in Fig. 1c.

$I(\lambda)$ used in Fig. 1b and in further analysis was calculated using a HALOE O_3 climatology (Grooß and Russell, 2005) and CLaMS photolysis code (Becker et al., 2000) for an altitude of 18.4 km (corresponding to the flight altitude of the RECONCILE self-match flight, cf. Sect. 3.1). To compare the ClO rises resulting from the considered photolysis rates with ClO observed during the self-match flight, we use the overall J_{ClOOCl} effective in the atmosphere obtained by integration of the areas under the curves plotted in Fig. 1c.

3 Experiment description

3.1 The self-match flight

The idea behind a self-match flight is to sample the same air masses twice during outbound and inbound flight legs of the same flight as has been described by Schofield et al. (2008). The flight was carried out on 30 January 2010 from Kiruna (67° 49′ N, 20° 20′ E), Sweden, as part of the large aircraft field campaign within the European project RECONCILE (von Hobe et al., 2011), employing the Russian research aircraft M-55 Geophysica with a ceiling altitude of 20 km. Flight track and match-pair trajectories are shown in Fig. 2.

To analyse the SZA dependence of J_{ClOOCl}, the flight was carried out over sunrise, with the first measurements still in darkness (i.e. with no active photolysis reactions and the chemical system expected to be in thermal equilibrium), and the second "matching" measurement in daylight, moving from higher to lower solar zenith angles (i.e. increasing solar radiation and photolysis rates) over the course of the inbound flight leg as is shown in Fig. 2. This was achieved by a nearly sun-synchronous flight pattern in westward direction for the outbound flight leg and the inbound flight leg coming

Title Page

Abstract | Introduction

Conclusions | References

Tables | Figures

⏮ | ⏭

◀ | ▶

Back | Close

Full Screen / Esc

Printer-friendly Version

Interactive Discussion

CC BY

ClOOCl photolysis at high solar zenith angles

O. Sumińska-Ebersoldt et al.

back in eastward direction. Location and timing of the flight were planned as to direct the aircraft into a region of elevated ClO_x. This was identified prior to the flight using the chemistry-transport model CLaMS (see Sect. 3.3) in the forecast mode. Air mass trajectories for the motion of individual air parcels between the two encounters were calculated based on data from the European Centre for Medium-Range Weather Forecasts (ECMWF).

3.2 Measurements

Chlorine monoxide (ClO) was measured by the HALOX (HALogen OXide monitor) instrument situated in a pod underneath the left wing of the Geophysica aircraft (von Hobe et al., 2005). Through an inlet optimised for radical measurements, ambient air is pumped through two measurement ducts where periodically (10 s cycles) NO is added, converting ClO to Cl atoms that are detected downstream by resonance fluorescence in the vacuum UV. HALOX has a detection limit of 5 ppt and an accuracy of about 18 %. Most critical for the analysis presented below is precision, which varies between 4 % and 8 % depending on the stability of the light source (helium discharge lamps containing chlorine) and on the observed detector noise. Random noise is reduced and signal-to-noise-ratio increased by integrating the signal over six NO addition cycles, yielding a time resolution of 1 min.

Temperature and pressure were measured using commercial Rosemount sensors and geolocation data were provided by the M-55 avionic system.

To examine the accuracy of matches (cf. Sect. 4.1), we used measurements of nitrous oxide (N_2O), which is expected to be unaffected by chemical processes on the time scale of the self-match flight and thus should show conserved mixing ratios. N_2O was measured by the 2-channel gas chromatograph HAGAR (High Altitude Gas Analyser, Volk et al., 2000) with a time resolution of 90 s. Mean precision and accuracy are better than 1 % and 2 % of the tropospheric background value, respectively.

Number concentrations of the particles with diameters of 6 nm, 11 nm and 15 nm were measured by COPAS (COndensation PArticle Counting System; Weigel et al.,

2009), which consists of an aerosol inlet and two dual-channel continuous flow Condensation Particle Counters (CPCs). The particles are detected in three channels operated with distinct temperature differences between the saturator and the condenser block. An other channel is operated with an aerosol heating line for a determination of the number of non-volatile particles. In the COPAS data, the exhaust gases of Geophysica were observed several times on the inbound flight leg confirming the good performance of the self-match flight.

3.3 CLaMS simulations

To define the match trajectories and to compare the ClO observations to values expected from various combinations of kinetic parameters, the Chemical Lagrangian Model of the Stratosphere (CLaMS) (McKenna et al., 2002a,b; Grooß et al., 2005) was used in a box-trajectory model mode, with trajectory calculations based on ECMWF wind fields and temperatures.

94 match trajectory start points were defined by the one-minute time intervals at which ClO was measured on the outbound flight leg. Forward trajectories were calculated until 12:00 UTC of 30 January with 1 min time resolution. The points with the lowest distance to the inbound flight track were then defined as pairing match points (cf. Sect. 4.1).

Chemistry calculations were also carried out on these trajectories with various combinations of J_{ClOOCl}, k_{rec} and K_{eq} values (cf. Sect. 4.4). For initialisation of the chemistry calculations, trace gas mixing ratios measured on the Geophysica (full list of sampled species published by von Hobe et al., 2011) during the outbound flight leg where used. Species not measured were taken from two-day back trajectory calculations initialised from a full hemispheric CLaMS simulation over the entire winter. The analysis of the backward trajectories revealed that the investigated air masses had been in darkness longer than 15 h prior to the flight, justifying the assumption of thermal equilibrium for the outbound flight leg (von Hobe et al., 2005). During these 15 h, temperature did not fall below 196.6 K on any of the trajectories, ruling out significant contribution of ClO

rise from Cl_2 released during very recent heterogeneous activation.

4 Results

4.1 Matches

Match points on the inbound flight leg corresponding to those on the outbound leg were found by minimising the horizontal radius around the coordinates of the Geophysica track and finding the coordinates fitting in time on the CLaMS forward trajectories. As shown in Fig. 3, the match radii R_{match} were always smaller than 8.5 km. To define a successful match pair, the vertical difference, in terms of potential temperature, between the locations of observations on the out- and inbound flight parts $\Delta\Theta$ also needs to be examined. Here, we only consider matches with $\Delta\Theta < 2.0$ K. The vertical ClO gradient measured during descent was 15 ppt K^{-1}.

To further test the accuracy of the matches, observations of the long-lived tracer N_2O by the HAGAR instrument were used. Match pairs, in which the difference between N_2O measured on the outbound and inbound flight legs was larger than the precision of HAGAR for the relevant data points (≈ 1.6 ppb), were rejected. With few exceptions, the tracer measurements confirmed an excellent match performance (Fig. 3, lower panel), as do several encounters of the Geophysica exhaust on the inbound flight leg identified by COPAS observations.

41 match pairs fulfilled all the conditions and are marked by large black circles in Fig. 3.

4.2 Night-time ClO_x chemistry

Figure 4 shows ClO_x mixing ratios calculated from the night-time ClO measurements and K_{eq} published by Plenge et al. (2005), Ferracci and Rowley (2010) and taken from JPL 2009 (Sander et al., 2009). An upper limit for ClO_x is given by the total inorganic

Title Page

Abstract | Introduction

Conclusions | References

Tables | Figures

|◄ | ►|

◄ | ►

Back | Close

Full Screen / Esc

Printer-friendly Version

Interactive Discussion

chlorine Cl_y, which was obtained from the tracer-tracer correlation with N_2O published by Grooß et al. (2002). The N_2O increase of 2.4 % over the past 10 yr was taken into account while no significant change in stratospheric Cl_y was assumed.

$$Cl_y = 3.394 + 0.001648 \cdot N_2O - 7.659^{-5} \cdot N_2O^2 + 2.646^{-7} \cdot N_2O^3 - 4.469^{-10} \cdot N_2O^4 \qquad (3)$$

N_2O and Cl_y are given in ppb and the relation is valid for N_2O values between 17–320 ppb.

Only the K_{eq} from Plenge et al. (2005) is consistent with observed night-time ClO. K_{eq} taken from studies of Ferracci and Rowley (2010) and JPL 2009 would result in ClO_x exceeding Cl_y. Therefore in our study K_{eq} from Plenge et al. (2005) is used to estimate ClOOCl for the further analysis.

4.3 Constraints on J_{ClOOCl} from the observed increase in ClO

The overall rate of change in ClO concentration resulting from the reactions system (R1)–(R4) is given by:

$$0.5 \frac{d[ClO]}{dt} = J_{ClOOCl}[ClOOCl] + k_{diss}[M][ClOOCl] - k_{rec}[M][ClO]^2 \qquad (4)$$

Figure 5 illustrates the SZA dependence of J_{ClOOCl} for the σ_{ClOOCl} i–iv for the conditions encountered during the RECONCILE self-match flight. The ClOOCl photolysis term is zero in darkness and rises more or less sharply, depending on the choice of σ_{ClOOCl}, as SZA decreases. Also shown is the ClOOCl thermal decomposition rate constant $k_{diss}[M]$ for the mean temperature and pressure observed during the flight. In thermal equilibrium, the rate of ClO production from this process is expected to equal the removal rate via the ClO self-reaction, i.e. $k_{diss}[M][ClOOCl] = k_{rec}[M][ClO]^2$ and $d[ClO]/dt = 0$. Thus, when the sun rises, ClO mixing ratios are expected to increase as soon as J_{ClOOCl} becomes large enough so that the photolysis reaction presents a significant additional ClO production term compared to the ClOOCl thermal decomposition. This point occurs at different SZA for the different σ_{ClOOCl} tested and can be compared to the SZA when a significant rise of ClO mixing ratios is actually observed.

Figure 6 shows that observed ClO starts to rise close to a SZA of 92°. Also shown is the simulated rise in ClO expected for the photolysis rates i–iv. This was calculated making two assumptions: [ClOOCl] is assumed to remain constant at its night-time concentration (calculated from observed night-time ClO concentrations and K_{eq} according to Plenge et al., 2005), and ClO removal from the self-reaction (Reaction R1) is ignored. Strictly, these assumptions hold true only at sunrise, i.e. when the first ClOOCl molecule is photolysed. As SZA decreases, [ClOOCl] will become smaller and ClO removal via the self-reaction faster, both leading to a reduced overall rate of ClO increase. Thus, the observed ClO increase and the integrated simulated ClO increase from ClOOCl photolysis are expected to start rising simultaneously at the threshold SZA with the observations then falling more and more below the theoretical line as SZA decreases.

Simulated ClO rise calculated for i) (scaled absorption spectra published by Pope et al., 2007) increases too late and proceeds too slow when compared with observed ClO. On the other end of the spectrum, a significant ClOOCl absorption band in the visible (case iv) would lead to an even earlier increase in ClO and is thus not warranted based on our observations. J_{ClOOCl} values based on ii) and iii) produce a reasonably good agreement between observed and expected ClO rise within the given uncertainties. They can probably be regarded as maximum and minimum of plausible photolysis cross sections effective in the atmosphere.

4.4 Chemistry simulations along match trajectories

In this analysis, box model runs with full chemistry calculations are initialised with the measurements made on the outbound flight leg. For calculation of ClOOCl mixing ratios, HALOX ClO and K_{eq} from the publication of Plenge et al. (2005) are used (cf. Sect. 4.2). The data sets resulting from the chemistry simulation runs along the trajectories between the points on the outbound and the inbound flight leg are compared with values observed on the inbound flight leg. The results are shown in Fig. 7.

Simulations were carried out for combinations of the four J_{ClOOCl} parametrisations discussed above and two parametrisations of k_{rec} (JPL 2009 and Nickolaisen et al., 1994). K_{eq} was taken from Plenge et al. (2005) (cf. Sect. 4.2).

Irrespective of the agreement between modelled and observed ClO, Fig. 7 illustrates the point made earlier, that immediately after sunrise, ClO mixing ratios are much more sensitive towards J_{ClOOCl} than towards k_{rec}. Only as the sun rises higher and ClO builds up, the influence of k_{rec} becomes important. Clearly, at high SZA at sunrise, the steady state approximation $J_{ClOOCl}/k_{rec} \approx [ClO]^2/[ClOOCl]$ is not valid.

In agreement with the results presented in Sect. 4.3, for the scaled cross sections of Pope et al. (2007), simulated ClO falls below observed mixing ratios as soon as they start to rise. In case ii), the model consistently follows the observations at very high SZA over sunrise, but predicts significantly smaller ClO mixing ratios than observed as SZA decreases further and photochemical steady state is approached. At these relatively low SZAs, simulations iii) and iv) show relatively good agreement with the observations, but they overestimate ClO earlier, especially cross section iv) with the artificial absorption band in the visible.

Provided that there are no additional reactions other than Reactions (R1)–(R4) governing the ClO-dimer cycle, the differences between model and observations for cases i) and iv) are too large for the underlying cross sections to be realistic in the atmosphere. For cases ii) and iii), the behaviour of the scaled von Hobe et al. (2009) parametrisation underestimating observed ClO at SZA < 90° and Papanastasiou et al. (2009) overestimating ClO at SZA > 90°, suggests ClOOCl cross sections within the range between those two. The HALOX measurements indicate an SZA threshold of significant ClO increase due to ClOOCl photolysis between 91.5° and 92° (cf. Fig. 6). That rules out the exponential extrapolation of σ_{ClOOCl} of Papanastasiou et al. (2009), because of its moderate slope at wavelengths larger than 350 nm, which would cause more than observed ClOOCl photolysis at too high solar zenith angles. The spectrum fully fitting our observed data is supposed to have the steep slope and shape of von Hobe et al. (2009) spectrum, but the scaling should be higher providing larger

photolysis at $\lambda < 350$ nm.

5 Conclusions

ClO measurements during the RECONCILE self-match flight on 30 January 2010 were used to examine the plausibility of published ClOOCl absorption cross sections measured in the laboratory and to test the hypothesis of an additional ClOOCl absorption in the visible. The analysis of the increase in ClO concentration over sunrise as well as CLaMS chemistry simulations suggest a ClOOCl photolysis frequency in the range resulting from absorption cross sections published by von Hobe et al. (2009) scaled to Lien et al. (2009) and by Papanastasiou et al. (2009). Cross sections published by Pope et al. (2007) are clearly inconsistent with our observations unless there are additional unknown processes converting ClOOCl to ClO in the atmosphere. The observed behaviour of ClO mixing ratios starting to increase only at SZA below 92° also rules out an additional absorption band of ClOOCl at wavelengths > 420 nm.

Additionally, the analysis of night-time ClO indicates that our observations are inconsistent with equilibrium constants higher than K_{eq} published by Plenge et al. (2005).

References

Becker, G., Grooß, J. U., McKenna, D. S., and Müller, R.: Stratospheric photolysis frequencies: impact of an improved numerical solution of the radiative transfer equation, J. Atmos. Chem., 37, 217–229, 2000. 18907

Birk, M., Friedl, R. R., Cohen, E. A., Pickett, H. M., and Sander, S. P.: The rotational spectrum and structure of chlorine peroxide, J. Chem. Phys., 91, 6588–6597, doi:10.1063/1.457377, 1989. 18904

Bloss, W. J., Nickolaisen, S. L., Salawitch, R. J., Friedl, R. R., and Sander, S. P.: Kinetics of the ClO self-reaction and 210 nm absorption cross section of the ClO dimer, J. Phys. Chem. A, 105, 11226–11239, doi:10.1021/jp012429y, 2001. 18904

Burkholder, J. B., Orlando, J. J., and Howard, C. J.: Ultraviolet-absorption cross-sections of Cl_2O_2 between 210 and 410 nm, J. Phys. Chem., 94, 687–695, doi:10.1021/j100365a033, 1990. 18904, 18906

Chen, H. Y., Lien, C. Y., Lin, W. Y., Lee, Y. T., and Lin, J. J.: UV absorption cross sections of ClOOCl are consistent with ozone degradation models, Science, 324, 781–784, doi:10.1126/science.1171305, 2009. 18904

Chipperfield, M. P., Feng, W., and Rex, M.: Arctic ozone loss and climate sensitivity: updated three-dimensional model study, Geophys. Res. Lett., 32, L11813, doi:10.1029/2005GL022674, 2005. 18906

Cox, R. A. and Hayman, G. D.: The stability and photochemistry of dimers of the ClO radical and implications for Antarctic ozone depletion, Nature, 332, 796–800, doi:10.1038/332796a0, 1988. 18904

DeMore, W. B. and Tschuikow-Roux, E.: Ultraviolet spectrum and chemical reactivity of the ClO dimer, J. Phys. Chem., 94, 5856–5860, doi:10.1021/j100378a046, 1990. 18904

Drdla, K. and Müller, R.: Temperature thresholds for polar stratospheric ozone loss, Atmos. Chem. Phys. Discuss., 10, 28687–28720, doi:10.5194/acpd-10-28687-2010, 2010. 18902

Ferracci, V. and Rowley, M.: Kinetic and thermochemical studies of the ClO + ClO + M <=> Cl_2O_2 + M reaction, Phys. Chem. Chem. Phys., 12, 11596–11608, doi:10.1039/C0CP00308E, 2010. 18910, 18911

Frieler, K., Rex, M., Salawitch, R. J., Canty, T., Streibel, M., Stimpfle, R. M., Pfeilsticker, K., Dorf, M., Weisenstein, D. K., and Godin-Beekmann, S.: Toward a better quantitative understanding of polar stratospheric ozone loss, Geophys. Res. Lett., 33, L10812,

Title Page

Abstract | Introduction

Conclusions | References

Tables | Figures

|◄ | ►|

◄ | ►

Back | Close

Full Screen / Esc

Printer-friendly Version

Interactive Discussion

doi:10.1029/2005GL025466, 2006. 18906

Grooß, J.-U. and Russell III, James M.: Technical note: A stratospheric climatology for O_3, H_2O, CH_4, NO_x, HCl and HF derived from HALOE measurements, Atmos. Chem. Phys., 5, 2797–2807, doi:10.5194/acp-5-2797-2005, 2005. 18907

Grooß, J.-U., Günther, G., Konopka, P., Müller, R., McKenna, D. S., Stroh, F., Vogel, B., Engel, A., Müller, M., Hoppel, K., Bevilacqua, R., Richard, E., Webster, C. R., Elkins, J. W., Hurst, D. F., Romashkin, P. A., and Baumgardner, D. G.: Simulation of ozone depletion in spring 2000 with the Chemical Lagrangian Model of the Stratosphere (CLaMS), J. Geophys. Res.-Atmos., 107, 8295, doi:10.1029/2001JD000456, 2002. 18911

Grooß, J.-U., Günther, G., Müller, R., Konopka, P., Bausch, S., Schlager, H., Voigt, C., Volk, C. M., and Toon, G. C.: Simulation of denitrification and ozone loss for the Arctic winter 2002/2003, Atmos. Chem. Phys., 5, 1437–1448, doi:10.5194/acp-5-1437-2005, 2005. 18909

von Hobe, M.: Revisiting ozone depletion, Science, 318, 1878, doi:10.1126/science.1151597, 2007. 18906

von Hobe, M., Grooß, J.-U., Müller, R., Hrechanyy, S., Winkler, U., and Stroh, F.: A re-evaluation of the ClO/Cl_2O_2 equilibrium constant based on stratospheric in-situ observations, Atmos. Chem. Phys., 5, 693–702, doi:10.5194/acp-5-693-2005, 2005. 18908, 18909

von Hobe, M., Salawitch, R. J., Canty, T., Keller-Rudek, H., Moortgat, G. K., Grooß, J. U., Müller, R., and Stroh, F.: Understanding the kinetics of the ClO dimer cycle, Atmos. Chem. Phys., 7, 3055–3069, doi:10.5194/acp-7-3055-2007, 2007. 18904

von Hobe, M., Stroh, F., Beckers, H., Benter, T., and Willner, H.: The UV/Vis absorption spectrum of matrix-isolated dichlorine peroxide, ClOOCl, Phys. Chem. Chem. Phys., 11, 1571–1580, doi:10.1039/B814373K, 2009. 18904, 18906, 18913, 18914

von Hobe, M., Grooß, J.-U., Pope, F., Peter, T., Cairo, F., Orsolini, I., Volk, C., Marchand, M., Janosi, I., Schlager, H., Stroh, F., Rex, M., Wienhold, F., and RECONCILE-Team: Reconciliation of essential process parameters for an enhanced predictability of arctic stratospheric ozone loss and its climate interactions, Atmos. Chem. Phys., to be submitted, 2011. 18907, 18909

Huder, K. J. and DeMore, W. B.: Absorption cross sections of the ClO dimer, J. Phys. Chem., 99, 3905–3908, doi:10.1021/j100012a007, 1995. 18904

Jin, B., Chen, I. C., Huang, W. T., Lien, C. Y., Guchhait, N., and Lin, J. J.: Photodissociation cross section of ClOOCl at 330 nm, J. Phys. Chem. A, 114, 4791–4797, doi:10.1021/jp909374k, 2010. 18904

Title Page

Abstract | Introduction

Conclusions | References

Tables | Figures

◄ | ►

◄ | ►

Back | Close

Full Screen / Esc

Printer-friendly Version

Interactive Discussion

Kaledin, A. L. and Morokuma, K.: An ab initio direct-trajectory study of the photodissociation of ClOOCl, J. Chem. Phys., 113, 5750–5762, doi:10.1063/1.1290606, 2000. 18904

Kremser, S., Schofield, R., Bodeker, G. E., Connor, B. J., Rex, M., Barret, J., Mooney, T., Salawitch, R. J., Canty, T., Frieler, K., Chipperfield, M. P., Langematz, U., and Feng, W.: Retrievals of chlorine chemistry kinetic parameters from Antarctic ClO microwave radiometer measurements, Atmos. Chem. Phys., 11, 5183–5193, doi:10.5194/acp-11-5183-2011, 2011. 18906

Lien, C. Y., Lin, W. Y., Chen, H. Y., Huang, W. T., Jin, B., Chen, I. C., and Lin, J. J.: Photodissociation cross sections of ClOOCl at 248.4 and 266 nm, J. Chem. Phys., 131(17), 174301, doi:10.1063/1.3257682, 2009. 18904, 18905, 18906, 18914

McElroy, M. B., Salawitch, R. J., Wofsy, S. C., and Logan, J. A.: Reductions of Antarctic ozone due to synergistic interactions of chlorine and bromine, Nature, 321, 759–762, doi:10.1038/321759a0, 1986. 18903

McKenna, D. S., Grooß, J. U., Günther, G., Konopka, P., Müller, R., Carver, G., and Sasano, Y.: A new Chemical Lagrangian Model of the Stratosphere (CLaMS) – 2. Formulation of chemistry scheme and initialization, J. Geophys. Res.-Atmos., 107, 4256, doi:10.1029/2000JD000114, 2002a. 18909

McKenna, D. S., Konopka, P., Grooß, J. U., Günther, G., Müller, R., Spang, R., Offermann, D., and Orsolini, Y.: A new Chemical Lagrangian Model of the Stratosphere (CLaMS) – 1. Formulation of advection and mixing, J. Geophys. Res.-Atmos., 107, 4309, doi:10.1029/2000JD000113, 2002b. 18909

Molina, L. T. and Molina, M. J.: Production of Cl_2O_2 from the self-reaction of the ClO radical, J. Phys. Chem., 91, 433–436, 1987. 18902

Nickolaisen, S. L., Friedl, R. R., and Sander, S. P.: Kinetics and mechanism of the Clo + Clo reaction – pressure and temperature dependences of the bimolecular and termolecular channels and thermal-decomposition of chlorine peroxide, J. Phys. Chem., 98, 155–169, doi:10.1021/j100052a027, 1994. 18913

Papanastasiou, D. K., Papadimitriou, V. C., Fahey, D. W., and Burkholder, J. B.: UV absorption spectrum of the ClO dimer (Cl_2O_2) between 200 and 420 nm, J. Phys. Chem. A, 113, 13711–13726, doi:10.1021/jp9065345, 2009. 18902, 18904, 18906, 18913, 18914

Peterson, K. A. and Francisco, J. S.: Does chlorine peroxide absorb below 250 nm?, J. Chem. Phys., 121, 2611–2616, doi:10.1063/1.1766012, 2004. 18904

Plenge, J., Kuhl, S., Vogel, B., Müller, R., Stroh, F., von Hobe, M., Flesch, R., and Ruhl, E.: Bond

Title Page

Abstract | Introduction

Conclusions | References

Tables | Figures

|◄ | ►|

◄ | ►

Back | Close

Full Screen / Esc

Printer-friendly Version

Interactive Discussion

strength of chlorine peroxide, J. Phys. Chem. A, 109, 6730–6734, doi:10.1021/jp044142h, 2005. 18902, 18910, 18911, 18912, 18913, 18914, 18924

Pope, F. D., Hansen, J. C., Bayes, K. D., Friedl, R. R., and Sander, S. P.: Ultraviolet absorption spectrum of chlorine peroxide, ClOOCl, J. Phys. Chem. A, 111, 4322–4332, doi:10.1021/jp067660w, 2007. 18902, 18904, 18906, 18912, 18913, 18914

Sander, S. P., Friedl, R. R., Barker, J. R., Golden, D. M., Kurylo, M. J., Wine, P. H., Abbatt, J., Burkholder, J. B., Kolb, C. E., Moortgat, G. K., Huie, R. E., and Orkin, V. L.: Chemical kinetics and photochemical data for use in atmospheric studies evaluation number 16: supplement to evaluation 15: update of key reactions, JPL Publication, Jet Propulsion Laboratory, Pasadena, CA, USA, 2009. 18910

Santee, M. L., Manney, G. L., Waters, J. W., and Livesey, N. J.: Variations and climatology of ClO in the polar lower stratosphere from UARS Microwave Limb Sounder measurements, J. Geophys. Res.-Atmos., 108, 4454–4454, doi:10.1029/2002JD003335, 2003. 18906

Schofield, R., Frieler, K., Wohltmann, I., Rex, M., von Hobe, M., Stroh, F., Koch, G., Peter, T., Canty, T., Salawitch, R., and Volk, C. M.: Polar stratospheric chlorine kinetics from a self-match flight during SOLVE-II/EUPLEX, Geophys. Res. Lett., 35, L01807, doi:10.1029/2007GL031740, 2008. 18906, 18907

Solomon, S., Garcia, R. R., Rowland, F. S., and Wuebbles, D.: On the depletion of Antarctic ozone, Nature, 321, 755–758, doi:10.1038/321755a0, 1986. 18902

Stimpfle, R. M., Wilmouth, D. M., Salawitch, R. J., and Anderson, J. G.: First measurements of ClOOCl in the stratosphere: the coupling of ClOOCl and ClO in the Arctic polar vortex, J. Geophys. Res.-Atmos., 109, D03301, doi:10.1029/2003JD003811, 2004. 18906

Toniolo, A., Granucci, G., Inglese, S., and Persico, M.: Theoretical study of the photodissociation dynamics of ClOOCl, Phys. Chem. Chem. Phys., 3, 4266–4279, doi:10.1039/b104044h, 2001. 18904

Tripathi, O. P., Godin-Beekmann, S., Lefevre, F., Marchand, M., Pazmino, A., Hauchecorne, A., Goutail, F., Schlager, H., Volk, C. M., Johnson, B., Konig-Langlo, G., Balestri, S., Stroh, F., Bui, T. P., Jost, H. J., Deshler, T., and von der Gathen, P.: High resolution simulation of recent Arctic and Antarctic stratospheric chemical ozone loss compared to observations, J. Atmos. Chem., 55, 205–226, doi:10.1007/s10874-006-9028-8, 2006. 18906

Volk, C., Riediger, O., Strunk, M., Schmidt, U., Ravegnani, F., Ulanovsky, A., and Rudakovand, V.: In situ tracer measurements in the tropical tropopause region during APE-THESEO, Eur. Comm. Air Pollut. Res. Report, 73, 661–664, 2000. 18908

Weigel, R., Hermann, M., Curtius, J., Voigt, C., Walter, S., Böttger, T., Lepukhov, B., Belyaev, G., and Borrmann, S.: Experimental characterization of the COndensation PArticle counting System for high altitude aircraft-borne application, Atmos. Meas. Tech., 2, 243–258, doi:10.5194/amt-2-243-2009, 2009. 18908

5   Wilmouth, D. M., Hanisco, T. F., Stimpfle, R. M., and Anderson, J. G.: Chlorine-catalyzed ozone destruction: Cl atom production from ClOOCl photolysis, J. Phys. Chem. A, 113, 14099–14108, doi:10.1021/jp9053204, 2009. 18904

Title Page

Abstract   Introduction

Conclusions   References

Tables   Figures

◄   ►

◄   ►

Back   Close

Full Screen / Esc

Printer-friendly Version

Interactive Discussion

Discussion Paper | Discussion Paper | Discussion Paper | Discussion Paper | Discussion Paper

ClOOCl photolysis at high solar zenith angles

O. Sumińska-Ebersoldt et al.
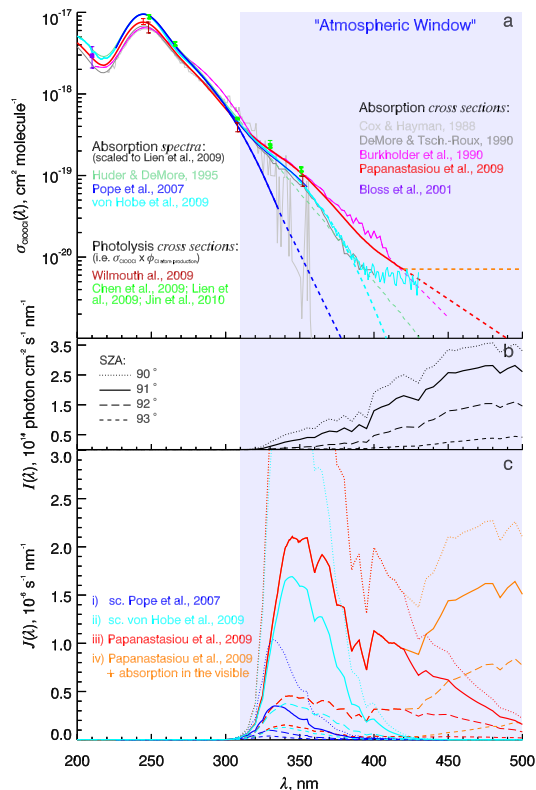
Fig. 1. Panel **(a)** presents a comparison of UV/Vis absorption spectra, absorption cross sections and photolysis cross sections of ClOOCl from various studies. The dashed extensions show the exponential extrapolation of chosen spectra in the actinic region. Spectra i–iv used in this study are shown with thicker lines, with the artificial spectrum for examination of the hypothesis of a ClOOCl absorption band in the visible represented by a dashed orange line. Panel **(b)** shows spectral actinic flux $I(\lambda)$ calculated for four solar zenith angles. The photolysis rate constants estimated for absorption cross sections i-iv and $I(\lambda)$ are shown in panel **(c)**.
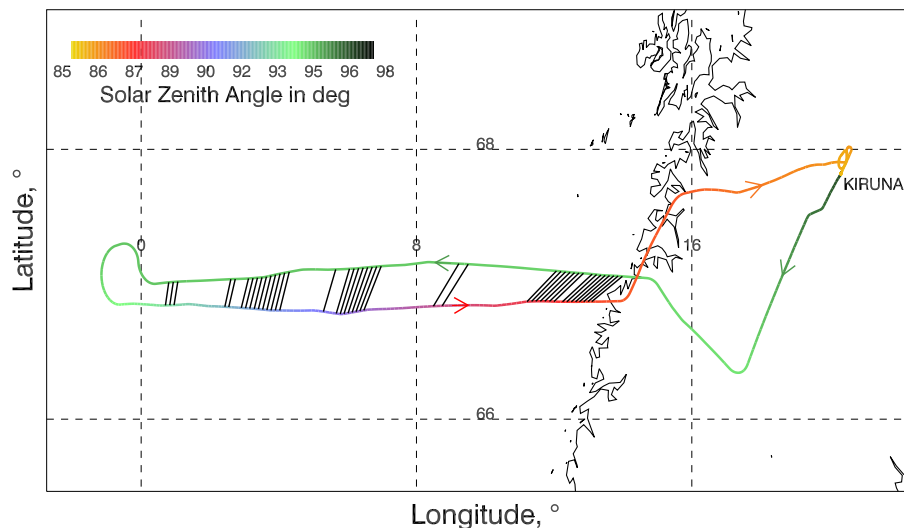
Fig. 2. Flight path of the RECONCILE self-match flight on 30 January 2010. The solar zenith angle on the track is represented by the colour scale. The black lines between outbound and inbound parts of flight represent the trajectories of the match pairs fulfilling the strict match conditions (cf. Sect. 4.1).
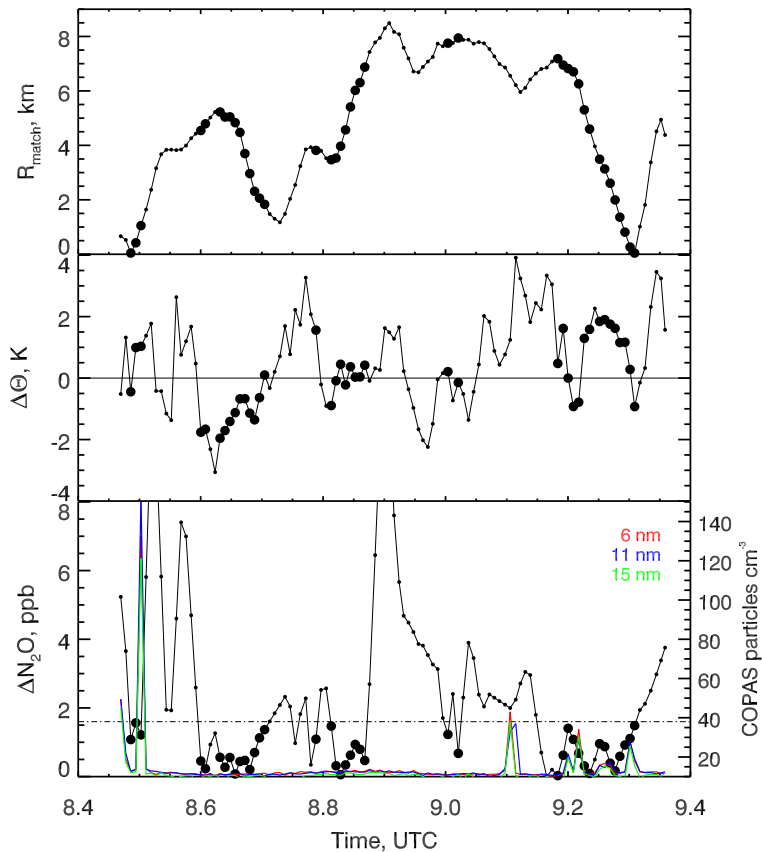
Fig. 3. Performance of the match-flight. The upper panel and the middle panels show the horizontal and the vertical match accuracy in form of match radii R_{match} (in km) and potential temperature difference $\Delta\Theta$ (in K), respectively. Differences in the mixing ratios of N_2O are shown in the lower panel. The red, blue and green lines correspond to the COPAS measurements. The increase of particle number concentrations indicates the Geophysica exhaust trail encounters.
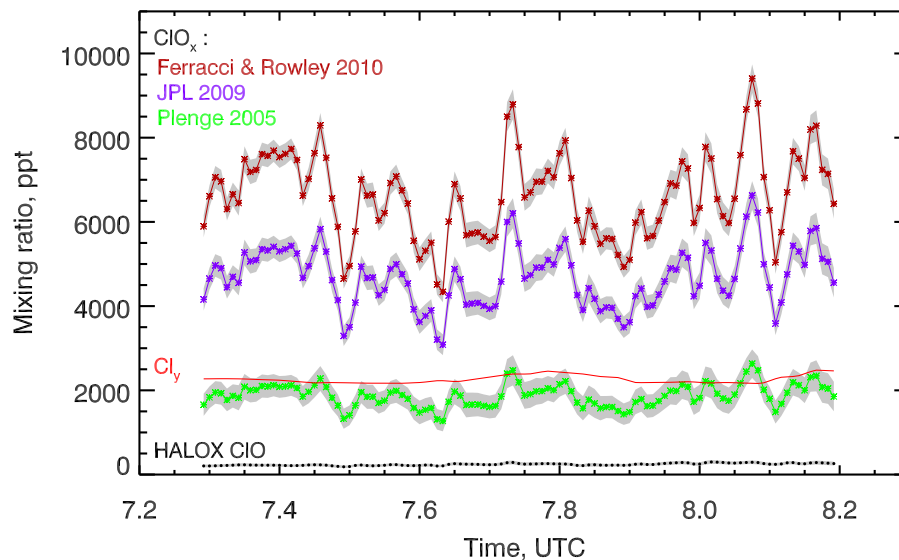
Fig. 4. ClO_x mixing ratios derived from HALOX ClO night measurements in combination with various K_{eq} parametrisations. The red line corresponds to Cl_y calculated from the correlation with N_2O (Eq. 3).

Title Page

Abstract | Introduction

Conclusions | References

Tables | Figures

◄ | ►

◄ | ►

Back | Close

Full Screen / Esc

Printer-friendly Version

Interactive Discussion

i)   sc. Pope et al., 2007
ii) sc. von Hobe et al., 2009
iii) Papanastasiou et al., 2009
iv) Papanastasiou et al., 2009
     + absorption in the visible
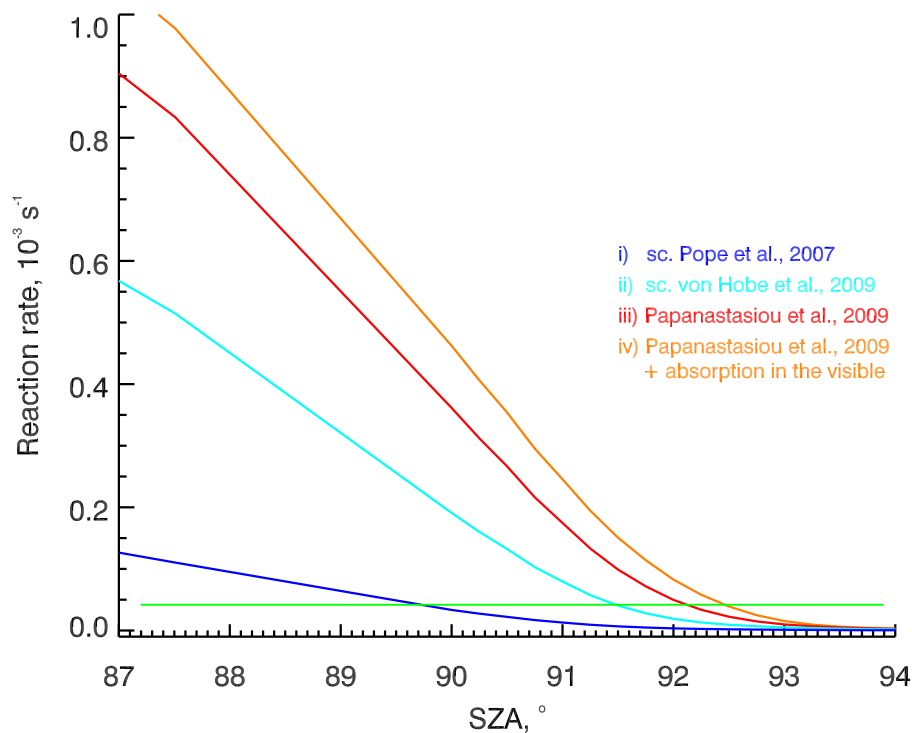
Fig. 5. Photolysis rate based on cross sections i–iv in dependence of solar zenith angle. The green line shows $k_{diss}[M]$ for comparison. k_{diss} was determined from the recombination constant taken from JPL 2009 and thermal equilibrium constant of Plenge et al. (2005). The number density [M] was calculated for the mean temperatures and pressure on the track of the Geophysica during the self-match flight.
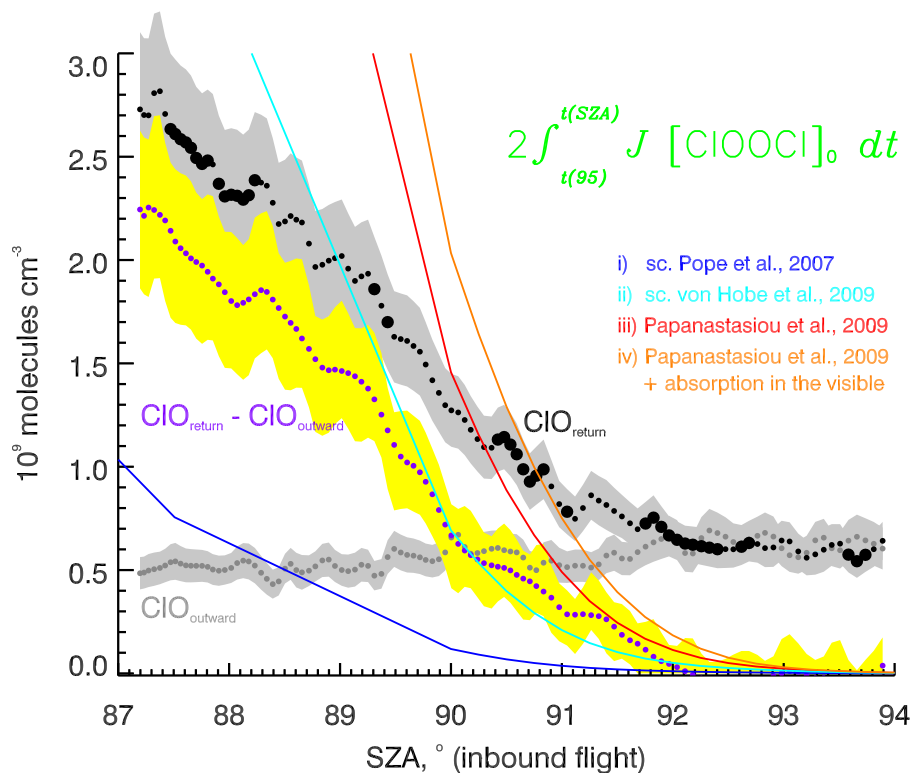
Fig. 6. Comparison of the observed rise of ClO concentrations (marked by the purple symbols) with SZA to the integrated ClO produced by simulations employing photolysis rates J_{ClOOCl} based on i–iv. The measured rise results from the subtraction of ClO measured on the outbound flight leg (grey symbols) from ClO measured on the inbound flight leg (shown as black symbols with the thicker ones representing strict match pairs). Grey and yellow areas show the measurement uncertainties.

Title Page

Abstract | Introduction

Conclusions | References

Tables | Figures

|◄ | ►|

◄ | ►

Back | Close

Full Screen / Esc
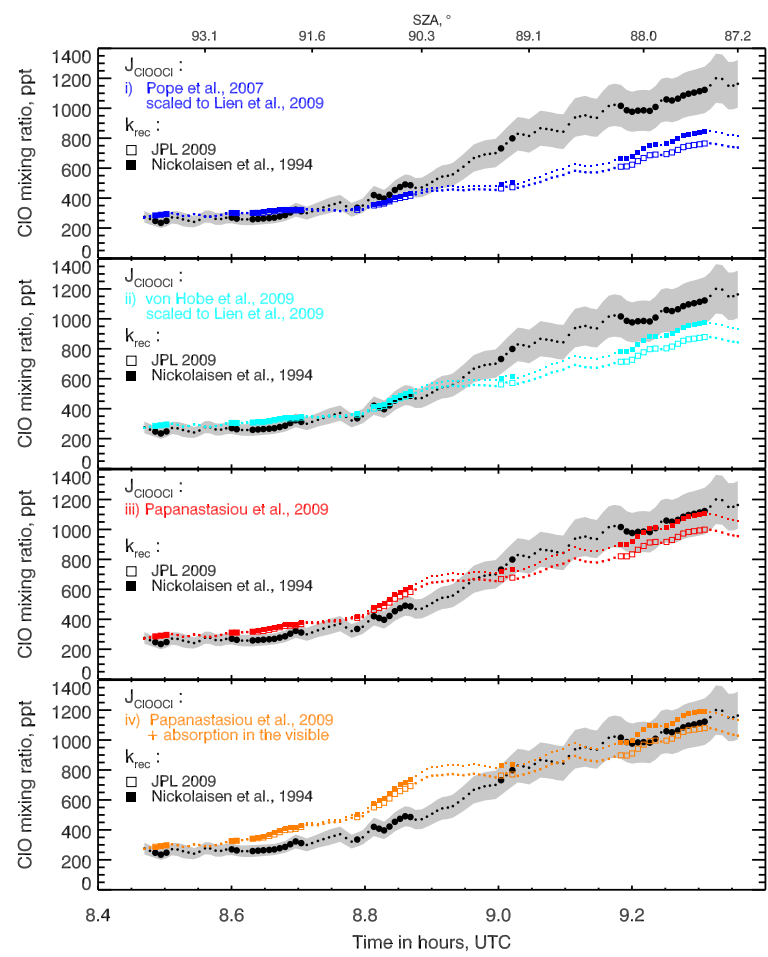
Printer-friendly Version

Interactive Discussion

Fig. 7. Comparison of HALOX ClO mixing ratio (black points with grey uncertainty areas) with the results of CLaMS simulations using various combinations of kinetic parameters. The "good matches" are marked with big symbols.